

Review Article

Fundamental Effects of Particle Morphology on Lung Delivery: Predictions of Stokes' Law and the Particular Relevance to Dry Powder Inhaler Formulation and Development

Timothy M. Crowder,¹ Jacky A. Rosati,² Jeffry D. Schroeter,³ Anthony J. Hickey,^{4,6} and Ted B. Martonen⁵

Received August 9, 2001; accepted November 29, 2001

Key factors that contribute to the aerodynamic properties of aerosol particles are found in Stokes' law. These factors may be monitored or controlled to optimize drug delivery to the lungs. Predictions of the aerodynamic behavior of therapeutic aerosols can be derived in terms of the physical implications of particle slip, shape and density. The manner in which each of these properties have been used or studied by pharmaceutical scientists to improve lung delivery of drugs is readily understood in the context of aerosol physics. Additional improvement upon current aerosol delivery of particulates may be predicted by further theoretical scrutiny.

KEY WORDS: aerosol(s); particles; Stoke's Law; density; shape; lung deposition.

INTRODUCTION

Dry powder inhalers (DPIs) continue to have an important role in delivering medicinal aerosols. A large number of DPI devices and technologies have been patented and published over the past decade (1,2). To effectively deliver a dose of medication, for either local or systemic action, DPI devices must overcome various physical obstacles (3). First, the small size of inhalable particles subjects them to forces of agglomeration and cohesion, resulting in poor flow and non-uniform dispersion. While larger excipient particles are frequently added to drug formulations to enhance their flow properties, separating the drug from the excipient requires an input of energy. In many DPI designs, shear forces created by turbulent airflow through the inhaler provide this energy.

The modern dry powder inhaler was first introduced in the 1960s with the Fisons Spinhaler[®] and Allen and Hanburys Rotahaler[®] (4). These devices operate by dispensing drug contained in a gelatin capsule, from either a spinning or rumbling motion, once the capsule has been opened by piercing

pins or cut by a plastic bar, respectively. The particles are dispersed through the turbulence generated by spinning blades or a plastic grid at the time of inhalation. Since the development of these early DPIs, a number of other dry powder inhalers have been designed with features ranging from self-contained metering systems and tortuous flow channels for particle deaggregation, to electronic dose counting systems.

Despite a relatively long history of development, the delivery of respirable drug particles to the lower airways and lungs by DPIs is still low. DPI performance varies widely by device and by flow rate through the device. A comparison of DPIs is given in Table I (35–39). The performance of these inhalers varies dramatically, though care must be taken in comparing values in the table as methods vary between authors and interdevice comparisons are complicated by widely varying resistances between devices. Dispersion of particles less than 6 to 7 μm ranges from around 10 to 35%. Although respirable percentage is of greater importance in the delivery of expensive biotechnology products, considerations of dose uniformity is common to all inhalation dosage forms.

There are physical principles governing the dynamics of fine particles dispersed as aerosols. These principles predict factors that could be employed to improve the deposition of respirable particles in the human lung. The aerodynamic drag force is the dominant factor in the dynamics of particles in air. The terminal settling velocity can be found by equating the force due to gravity and the aerodynamic drag force

$$mg = \frac{3\pi\mu dV}{C_c} \quad (1)$$

where m is the particle mass, g is the gravitational constant

¹ Department of Biomedical Engineering, University of North Carolina, Chapel Hill, North Carolina 27599.

² Department of Environmental Sciences and Engineering, University of North Carolina, Chapel Hill, North Carolina 27599.

³ Curriculum in Toxicology, University of North Carolina, Chapel Hill, North Carolina 27599.

⁴ School of Pharmacy and Dept of Biomedical Engineering, University of North Carolina, Chapel Hill, North Carolina 27599.

⁵ Experimental Toxicology Division, National Health and Environmental Effects Research Laboratory, University of North Carolina, Chapel Hill, North Carolina 27599.

⁶ To whom correspondence should be addressed. (email: ahickey@unc.edu)

Table I. Performance Comparison of Selected DPIs

DPI	Drug	Flow Rates (Lpm)	Cutoff for FPF (μm)	FPF (%)	Method	Reference
Spinhaler	Cromolyn sodium	60/120	na/na	5.5/13.1	Lung deposition <i>in vivo</i>	Newman (35)
	Cromolyn sodium	60/120	<6.8/<4.9	10.1/18.4	MSLI	Newman (35)
	Cromolyn sodium	60/90	<6.4/<5.2	10.1/22.7	TSI	Steckel (36)
Diskhaler	Cromolyn sodium	30/60	<9.9/<7	3.0/9.5	4-stage impactor	de Boer (37)
	Salbutamol	60/90	<6.4/<5.2	30.5/32.1	TSI	Steckel (36)
Turbuhaler	BDP	30/60	<9.9/<7.7	12.0/23.0	4-stage impactor	de Boer (37)
	Terbutaline	28/60	<5.8/<6.4	11.8/46.3	Andersen/TSI	Meakin (38)
Diskus	Budesonide	30/60	<9.9/<7	20.0/38.0	4-stage impactor	de Boer (37)
	Fluticasone	60	<6.4	25.4	TSI	Steckel (36)
Easyhaler	Salbutamol	60	<6.4	36.0	TSI	Steckel (36)
Clickhaler	Procaterol	60	<6.4	35.2	TSI	Fukunaga (39)

Fine particle fraction (FPF) is the percentage of particles less than the diameter used as the FPF cutoff diameter (column 4). Methods used for FPF measurement include *in vivo* deposition imaging, multi-stage liquid impinger (MSLI), twin stage impinger (TSI) and cascade impactors.

and $3\pi\mu dV$ is the Stokes' force where μ is the viscosity of air, d is the particle diameter, V is the particle velocity and C_c is the Cunningham slip correction factor. By solving for V and expressing the particle mass in terms of its mass density ρ_p the resulting equation gives the terminal settling velocity

$$V = \left(\frac{gC_c}{18\mu} \right) \rho_p d^2 \quad (2)$$

For non-spherical particles, a shape factor must be included in the equations above. The practical and theoretical implications of shape on aerodynamic properties have been discussed by a number of authors (5–7). For example, elongated particles have an aerodynamic diameter a few times smaller than their length. Although this would offer advantages for deep lung deposition, dispersion of the particles by an inhaler is difficult to achieve for elongated particles (8).

Porous particles have recently attracted attention for pulmonary deposition. The particles are engineered to be less than unit density by virtue of a porous structure with trapped air volume within the particle. Since these particles have a mass density significantly lower than unity, particles with an aerodynamic diameter (diameter of a unit density sphere with the same settling velocity as the particle in question) in the respirable size range can be achieved despite having a geometric particle size greater than 10 μm (9–11).

The physical implications of slip, shape and density on aerosol behavior will be discussed in the context of the delivery of therapeutic agents to the peripheral regions of the lungs. Potential options for the improvement of aerosol delivery of particles will be inferred from fundamental principles of aerosol physics.

AERODYNAMIC BEHAVIOR OF INHALED AEROSOLS

Slip Correction Factor

Stokes Law assumes that the relative velocity of a carrier gas at a particle's surface is zero; this assumption does not hold for small particles. A slip correction factor, derived by Cunningham and given in Eq. (3), should be applied to Stokes law for particles smaller than 10 microns.

$$C_c = 1 + Kn \left[A1 + A2 \exp\left(-\frac{A3}{Kn}\right) \right] \quad (3)$$

where Kn is the Knudsen Number, and $A1$, $A2$ and $A3$ are constants.

Values for $A1$, $A2$ and $A3$ are derived from experimental measurements of drag on small particles. While the values of these constants have varied slightly over the years, the most common values were determined by Davies in 1945 (12), and are given by Reist (7) and Hinds (13) as $A1 = 1.257$, $A2 = 0.4$ and $A3 = 1.1$.

The Knudsen number is a ratio of mean free path of the gas molecules to particle size (Eq. 4). It is dependent on heat, mass and momentum transfer between the particles and carrier gas.

$$Kn = \frac{2\lambda}{d} \quad (4)$$

where λ is mean free path of the gas molecules and d is the particle diameter. Mean free path can be calculated using Eq.(5):

$$\lambda = v \left(\frac{\pi m}{2kT} \right)^{1/2} \quad (5)$$

where v is the kinematic viscosity of the gas, m is the molecular mass, k is Boltzmann's constant, and T is the absolute temperature (14).

The Cunningham slip correction factor reduces the value of Stokes drag force. Stokes drag now takes the form given by Eq. (6):

$$F_D = \frac{3\pi\mu Vd}{C_c} \quad (6)$$

where μ is the viscosity of air, V is the particle velocity, and d is the particle diameter.

Table II shows how Stokes number changes for a unit density sphere of a given particle size using slip correction with the constants from Davies (12). Values given are calculated for 20 degrees C and 101 kPa. The slip correction factor also needs to be applied to particle settling velocity, V_{TS} , given by Eq. (7).

Table II. Effect of Cunningham Slip Correction Factor on Stokes Drag and Terminal Settling Velocity

Particle Diameter, microns	Cc	VTS (w/o Cc) cm/s	VTS (with Cc) cm/s
0.001	228.234	3.02E-09	6.61E-07
0.01	23.3443	3.02E-07	6.77E-06
0.1	2.97393	3.02E-05	8.71E-05
0.5	1.34743	7.54E-04	1.005E-03
1	1.17273	3.02E-03	3.516E-03
1.5	1.11514	6.79E-03	7.536E-03
2	1.08636	1.21E-02	1.306E-02
3	1.05757	2.71E-02	2.864E-02
5	1.03454	7.54E-02	7.790E-02
7	1.02467	1.48E-01	1.513E-01
10	1.01727	3.02E-01	3.066E-01

$$V_{TS} = \frac{\rho_p d_p^2 g C_c}{18\mu} \quad (7)$$

where ρ_p is the particle density, d_p is the particle diameter, and g is the acceleration due to gravity. Predicted particle settling velocity increases when a slip correction factor is applied (Table II, Columns 3, 4). Note the drastic difference between the corrected and uncorrected velocity values for submicron particles. On a 0.001 micron particle, drag force decreases by a magnitude of 228 and, thus, terminal settling velocity increases by a magnitude of 228 when a slip correction factor is utilized. Thus, it is very important to correct for slip when calculating the settling velocity of small particles (<1 micron). For a more thorough understanding of these equations, the reader is referred to aerosol physics texts such as Hinds (13).

Particle Density

Particle density is an important parameter in aerosol physics. Of primary interest is its use in the calculation of a particle’s aerodynamic diameter. The aerodynamic diameter of a particle, or d_{ae} , is the diameter of a unit density sphere that has the same settling velocity as the particle in question. d_{ae} can be calculated using Eq. (8).

$$d_{ae} = \sqrt{\rho_p} d_g \quad (8)$$

where ρ_p is the particle density and d_g is the particle’s geometric diameter. Table III shows how geometric diameter varies with particle density at a given aerodynamic diameter.

The use of large geometric diameter, low-density particles is being explored as a means of improving the delivery of inhaled therapeutics. Interestingly, nature itself has developed the classic large diameter, low-density particle in the form of pollen. Figure 1 is a photomicrograph of a common pollen, Ragweed. One can see the spherical base with conical protrusions from the surface. Yet, despite Ragweed pollen’s irregular shape, it is very effective at depositing in the human airways.

Non-Spherical Particles

When particles are non-spherical, a dynamic shape correction factor must be applied to Stokes law. This factor corrects for the effect of shape irregularity on drag force and

Table III. Aerodynamic Diameter and Corresponding Geometric Diameter Variation with Particle Density

d_{ae} (microns)	Density, ρ (grams/cc)	d_g (microns)
0.1	0.1	0.3162
	1.0	0.1
	1.5	0.0816
1	0.1	3.1623
	1.0	1
	1.5	0.8165
3	0.1	9.4868
	1.0	3
	1.5	2.4495
5	0.1	15.8114
	1.0	5
	1.5	4.0825

terminal settling velocity. Eq. (9) shows terminal settling velocity corrected for particle shape.

$$V_{TS} = \frac{\rho_p d_e^2 g C_c}{18\mu X} \quad (9)$$

where d_e is the equivalent volume diameter and X is the dynamic shape correction factor. The equivalent volume diameter is the diameter of a spherical particle that is equivalent in volume to the non-spherical particle in question, and can be determined experimentally (15).

Eq. (10) shows aerodynamic diameter corrected for shape:

$$d_{ae} = d_e \left(\frac{\rho_p}{X} \right)^{1/2} \quad (10)$$

While the derivation of shape correction factors is beyond the scope of this paper, the implications of shape on aerodynamic properties have been discussed by a number of authors (13,16–18). Table IV provides dynamic shape factors for common particle shapes and types (13).

Deposition in the Lung

Particle deposition in the lung is governed primarily by three mechanisms: Impaction, Sedimentation and Diffusion. Particle slip, shape and density affect deposition of particles in

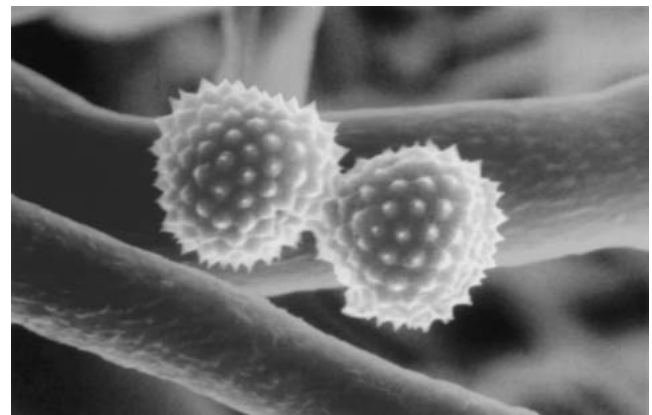


Fig. 1. Ragweed Pollen (Photo Courtesy of Johnny L. Carson). Ragweed pollen particles generally range from 16 to 27 μm in size.

Table IV. Dynamic Shape Factors for Common Particle Shapes and Types

Shape	Dynamic Shape Factor, X
Sphere	1.00
Cube	1.08
Cylinder ($L/D = 2$) horizontal axis	1.14
Cylinder ($L/D = 2$) vertical axis	1.01
Straight Chain ($L/D = 2$)	1.10
Sand	1.57
Talc	1.88

the human lung by contributing to at least one of the above mechanisms.

Particle deposition from inertial impaction and sedimentation is directly dependent upon τ , the relaxation time of the aerosol particle (19). Eq. (11) defines relaxation time:

$$\tau = \frac{d_p^2 \rho_p}{18\mu} C_c = \frac{d_{ae}^2 \rho_o}{18\mu} C_c \quad (11)$$

where d_p is particle diameter, ρ_p is particle density, d_{ae} is aerodynamic particle diameter and ρ_o is unit density (13). Recall that aerodynamic diameter is dependent upon both density and shape of a particle, as seen in Eqs. (8) and (10). From Eq. (11), relaxation time has a direct relationship with the slip correction factor.

Particle deposition from diffusion is directly dependent on the Diffusion Coefficient, D , defined by Eq. (12).

$$D = \frac{C_c kT}{3\pi\mu d_g} \quad (12)$$

From Eq. (12), the Diffusion Coefficient has a direct relationship with the slip correction factor. Thus, from Eqs. (11) and (12), we see the importance of slip, density and shape on deposition of particles in the human lung. Without correction for these factors, calculation of aerodynamic particle properties and deposition probabilities would be inaccurate.

PHARMACEUTICAL IMPLICATIONS

Slip

Slip correction becomes significant for pharmaceutical particles less than 1 μm and is most significant for particles less than 0.1 μm (the slip correction value increases from 1.16 at 1 μm to 2.9 at 0.1 μm) (7). In general, particles less than about 0.5 μm will be exhaled from the lungs without depositing (20). The distribution of particle sizes that comprise a pharmaceutical aerosol is a major factor affecting the spatial distribution of particle deposition in the lung since the mechanisms of deposition are dependent on particle size. Inhaled aerosols are typically described by lognormal size distributions that are defined by a mass median aerodynamic diameter (MMAD) and geometric standard deviation (GSD). While these parameters yield information on relative proportions of particle sizes, what may be more useful is the distri-

bution of mass, specifically the percentage of total mass from particles in the submicron range. For a fixed MMAD, the particle size range is highly influenced by the GSD. For example, for an MMAD of 1, as the GSD is increased from 1.5 to 2.5, the count median diameter (CMD) is decreased from 0.6107 to 0.0806, but the percentage of mass from submicron particles remains relatively constant at around 52%. For MMADs of 2 and 3, as the GSD increases from 1.5 to 2.5, the CMD decreases into the submicron range, guaranteeing that more than half of the particles are submicron in size. But even though the particle sizes may be clustered in the submicron range, a large proportion of the total mass may still come from the larger particles since mass is proportional to the cube of the particle diameter. For example, for an MMAD of 2, as the GSD increases from 1.5 to 2.5, the percentage of mass from submicron particles increases from 5.0% to 24.1%; for an MMAD of 3, as the GSD increases from 1.5 to 2.5, that percentage increases from 0.5% to 12.5%. Therefore, for aerosols with relatively small MMADs (around 1 μm), submicron particles may significantly contribute to pharmaceutical effect, but as MMAD increases, this effect is minimized. However, the above discussion relating to the percentage of submicron mass indicates that slip correction is not an irrelevancy for aerosol dosage forms.

Deposition models that include effects of Brownian motion have shown low deposition efficiency for particles less than 1 μm in the upper airways (21). Breath holding during the inhalatory maneuver increases the likelihood that particles deposit due to their increased residence time in the lungs. However, human studies with 1 μm aerosols in low and normal gravity conditions have demonstrated that gravitational sedimentation is the dominant mechanism of deposition during breath holding (22). The various domains of deposition mechanisms have been described by Heyder (23). For unit density particles, the "thermodynamic" domain where Brownian motion dominates deposition is for particles less than approximately 0.16 μm . From this diameter up to 1 μm , deposition is mixed between diffusion and sedimentation while impaction dominates for particles larger than 1 μm . The effect of particle size distribution on the mechanisms of deposition has also been addressed.

Shape

Fibers, discussed below for their medical implications, belong to a general class of rod-like particles, which because of their very shapes, have rather unusual airborne characteristics (24). It is very important, therefore, to classify fibers by their appropriate physical characteristics. The aerodynamic properties of individual fibers may be determined in terms of the length (L), diameter (D) and aspect ratio (L/D) of the particles (25). A key point is that the aerodynamic diameter of a fiber, D_{ae} , is relatively independent of its length, being proportional to $(L)^{1/6}$. Therefore, a fiber is ideally suited for transporting a relatively massive quantity of drug deeply into human lungs without adversely affecting its airborne behavior. Chan and Gonda developed elongated crystals of cromoglycic acid (8). Their particles had an average length of approximately 2 μm and an aspect ratio of 10 resulting in an MMAD of 0.7 μm as determined by cascade impaction. The proposed advantage of these particles is that deeper deposition results in more efficacious therapeutic effect (26). Similar

formulation and characterization has been performed for Nedocromil (27). The particles described in both of these studies were dispersed by nebulization. Unfortunately, dispersion of elongated particles as dry powders may be poor since they are subject to large attractive forces when in contact along their length (28).

An exciting new form of fiber has been generated in the laboratory, specifically for applications in the medical arena. Johnson *et al.* (34) have developed techniques to produce hollow microtubules with lipid bilayer membranes wound helically as a tubular structure. Recently, studies have been performed to ascertain the drug encapsulation features of these microtubules (29).

Another study utilizing particle morphology to influence deposition properties treated disodium chromoglycate (DSCG) with fatty acids (6). Treatment of DSCG with lauric, palmitic and stearic acids increased the fine particle fractions of doses delivered with a Rotahaler as determined by a twin impinger. The aerodynamic diameter was further studied via cascade impaction. The mechanism by which fine particle fraction was increased was proposed to be a decrease in the aerodynamic diameter of treated particles. Fatty acid treatment caused the DSCG particles to become elongated, thus decreasing their projected diameter. In the case of lauric acid treatment, the coating reduced particle interactions to increase dispersability.

When considering the motion of inhaled fibers, another mechanism of deposition (i.e., beyond inertial impaction, sedimentation and diffusion) is dominant. It is termed interception, and occurs when the center of mass of the particle stays on a fluid streamline but, due to the elongated shape, comes into physical contact with an airway's surface. The deposition process of interception has been explicitly formulated by Balashazy *et al.* (30) for application to airway bifurcations.

Density

There are at least two ways to achieve low-density particles. A porous matrix can be prepared, as illustrated in Fig. 2a, or hollow spheres can be produced, as shown in Fig. 2b. Recently, the development of large porous particles, characterized by their low mass density and large geometric size, has received attention as a potential option for the efficient delivery of therapeutic drugs to the alveolated airways (9,11). There is a potential to optimize pulmonary lung deposition through the engineering of large porous particles. For particles with a density less than 1 g/cm^3 , an aerodynamic diameter in the respirable size range can be achieved with a geometric particle size greater than $10 \text{ }\mu\text{m}$ (10). These particles disperse well from DPIs, and have been shown to improve peripheral (i.e., pulmonary or alveolar) lung deposition by reducing deposits in the extrathoracic (mouth and throat) and tracheobronchial airways, making them ideally suited for inhaled therapies used in the treatment of 'deep' lung diseases (e.g., cystic fibrosis), and systemic delivery (e.g., insulin). One element of their improved dispersion properties is the reduction of van der Waals forces essentially by inserting space (in the form of pores) between the point charges within the particle. This advantage is achieved at the expense of the total mass delivered by each particle and the need for optimization of density and volume (occupied by the powder and stored in

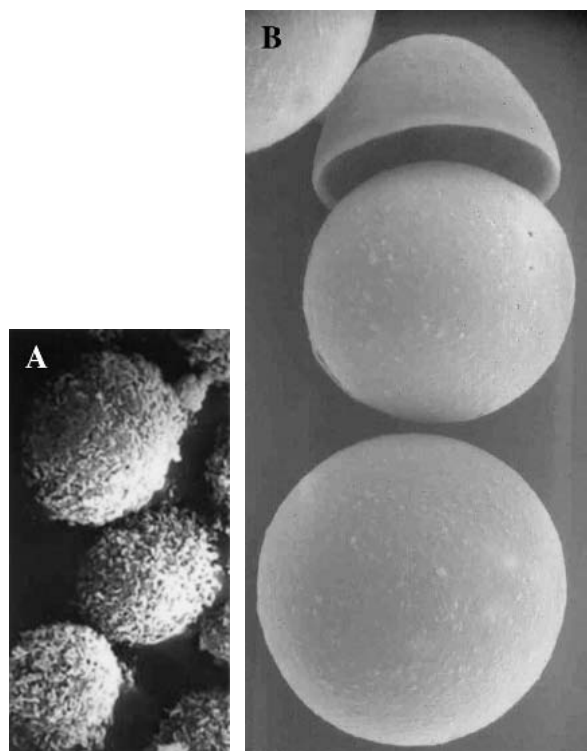


Fig. 2. Electron micrographs of a low density porous (A) and hollow sphere (B) particles. Although measurement bars were not available for these particular particles, their size is known to be less than $10 \text{ }\mu\text{m}$.

the dose package) to effectively deliver a therapeutic dose to the patient.

Hygroscopicity

Hygroscopic aerosols associate with moisture under defined conditions of temperature and relative humidity. This has implications for aggregation and dispersion of dry powders and for aerodynamic properties of particles in transit through the airways (19,31,32). Hygroscopic growth of pharmaceutical aerosols is a frequent occurrence (33). The overall effect of hygroscopic growth is to increase lung deposition. However, regional deposition is dependent upon the particle size of the aerosol entering the airways. It has been demonstrated that the presence of hydrophobic additives reduce the hygroscopic growth rate, the instantaneous particle size and by inference the deposition of aerosols in the lungs (34). The influence of particle size on the dynamics of the particle motion will clearly be affected by hygroscopic growth as the particles traverse the airways.

CONCLUSION

It is clear from this exposition that the fundamental characteristics of particles dictating their aerodynamic properties can be manipulated to achieve optimal behavior. Stokes' law identifies the characteristics that influence this behavior. Particle density, shape and size (including change in flow regime associated with particles $<1\text{ }\mu\text{m}$) play key roles in aerodynamic performance. This has been demonstrated to some extent in practical approaches to drug delivery. In addition, more subtle effects from features, such as surface asperities,

as demonstrated in Fig. 1, may arise. These surface features may be construed as 'surface porosity' or reduced 'surface density', consequently increasing the distance between particles while reducing the point charges. Thus, it is anticipated that van der Waals forces would be smaller, drag forces would be greater and dispersion properties would improve. This has the advantage of allowing a core solid particle (of large density) to be delivered efficiently, reducing concerns about dose limitations arising from completely porous or hollow particles.

The physical implications of Stokes' law govern the dynamics of aerosol particle movement. The variable terms in Stokes' law and their effect on particle dynamics have been reviewed. Examples have been presented to elucidate the manner in which these terms have been, or can be, manipulated to affect the deposition of pharmaceutical aerosol particles in the human airways. It is a humbling thought that Stokes (and van der Waals) stated clearly the limitations to particle behavior contributing to lung delivery of drugs more than a century before it was conceived.

DISCLAIMER

The information in this document has been funded wholly (or in part) by the U. S. Environmental Protection Agency. It has been subjected to review by the National Health and Environmental Effects Research Laboratory and approved for publication. Approval does not signify that the contents necessarily reflect the views of the Agency, nor does mention of trade names or commercial products constitute endorsement or recommendation for use.

ACKNOWLEDGMENTS

JD Schroeter was funded by the EPA/UNC Toxicology Research Program, Training Agreements CT902908 and CT827206, with the Curriculum in Toxicology, University of North Carolina at Chapel Hill.

References

1. A. J. Hickey and C. A. Dunbar. A New Millennium for Inhaler Technology. *Pharm. Tech.* **21**:116–125 (1997).
2. T. M. Crowder, M. D. Louey, V. V. Sethuraman, H. D. C. Smyth, and A. J. Hickey. 2001: An Odyssey in Inhaler Formulations and Design. *Pharm. Tech.* **25**:99–113 (2001).
3. D. Prime, P. J. Atkins, A. Slater, and B. Sumbly. Review of Dry Powder Inhalers. *Adv. Drug Deliver. Rev.* **26**:51–58 (1997).
4. A. R. Clark. Medical Aerosol Inhalers: Past, Present, and Future. *Aerosol Sci. Tech.* **22**:374–391 (1995).
5. I. Colbeck. Dynamic shape factors of fractal clusters of carbonaceous smoke. *J. Aerosol Sci.* **21**:S43–S46 (1990).
6. K. A. Fults, I. F. Miller, and A. J. Hickey. Effect of Particle Morphology on Emitted Dose of Fatty Acid-treated Disodium Cromoglycate Powder Aerosols. *Pharm. Dev. Technol.* **2**:67–79 (1997).
7. P. C. Reist. *Aerosol Science and Technology*. McGraw-Hill, New York, 1993.
8. H.-K. Chan and I. Gonda. Aerodynamic Properties of Elongated Particles of Cromoglycic Acid. *J. Aerosol Sci.* **20**:157 (1989).
9. D. A. Edwards, A. Ben-Jebria, and R. Langer. Recent Advances in Pulmonary Drug Delivery Using Large, Porous Inhaled Particles. *J. App. Physiology* **85**:379–385 (1998).
10. D. A. Edwards, D. Chen, J. Wang, and A. Ben-Jebria. Controlled-Release Inhalation Aerosols. *Respiratory Drug Deliver, V.I.R.N.* Dalby, P. R. Byron, S. J. Farr, Interpharm Press, Inc. Englewood, Colorado, 187–192 (1998).
11. D. A. Edwards, J. Hanes, G. Caponetti, J. Hrkach, A. Ben-Jebria, M. L. Eskew, J. Mintzes, D. Deaver, N. Lotan, and R. Langer. Large porous particles for pulmonary drug delivery. *Science* **276**:1868–1871 (1997).
12. C. N. Davies. Definitive equations for the fluid resistance of spheres. *Pro. Phys. Soc.* **57**:259–270 (1945).
13. W. C. Hinds. *Aerosol Technology: Properties, behavior and measurement of airborne particles*. Wiley, New York, 1999.
14. S. Friedlander. *Smoke, Dust and Haze: Fundamentals of Aerosol Dynamic*. Oxford University Press, New York, 1977.
15. K. Willeke and P. Baron. *Aerosol Measurement: Principles, Techniques and Applications*. Wiley, New York, 1997.
16. O. Moss. Shape factors for airborne particles. *Am. Ind. Hyg. Assoc. J.* **32**:221–229 (1971).
17. W. A. Stöber. A note on the aerodynamic diameter and the mobility of non-spherical aerosol particles. *J. Aerosol Sci.* **2**:453–456 (1971).
18. D. Leith. Drag on nonspherical object. *Aerosol Sci. Tech.* **6**:153–161 (1987).
19. T. B. Martonen, K. Bell, R. Phalen, A. Wilson, and A. Ho. Growth rate measurements and deposition modeling of hygroscopic aerosols in human tracheobronchial models. *Ann. Occ. Hyg.* **26**:93–108 (1982).
20. S. J. Smith and J. A. Bernstein. Therapeutic uses of lung aerosols. In A. J. Hickey (ed.), *Inhalation aerosols: Physical and Biologic basis for Therapy*, Marcel Dekker, Inc., New York, 1996, pp. 233–269.
21. A. Li and G. Ahmadi. Computer simulation of particle deposition in the upper tracheobronchial tree. *Aerosol Sci. Tech.* **23**:201–223 (1995).
22. C. Darquenne, M. Paiva, and G. K. Prisk. Effect of gravity on aerosol dispersion and deposition in the human lung after periods of breath holding. *J. App. Physiol.* **89**:1787–1792 (2000).
23. J. Heyder, J. Gebhart, G. Rudolf, C. F. Schiller, and W. Stahlhofen. Deposition of particles in the human respiratory tract in the size range 0.005–15 μm . *J. Aerosol Sci.* **17**:811–825 (1986).
24. R. L. Harris and D. A. Fraser. A model for deposition of fibers in the human respiratory system. *Am. Ind. Hyg. Assoc. J.* **37**:73–89 (1976).
25. T. B. Martonen and D. L. Johnson. Aerodynamic size classification of fibers with aerosol centrifuges. *Part. Sci. Technol.* **8**:37–53 (1990).
26. S. H. Curry, A. J. Taylor, S. Evans, S. Godfrey, and E. Zeidifard. Disposition of disodium chromoglycate administered in three particle sizes. *Brit. J. Clin. Pharm.* **2**:267–270 (1975).
27. H.-K. Chan and I. Gonda. *J. Aerosol Med.* **6**:241–249 (1993).
28. J. Visser. An invited review: Van der Waals and other cohesive forces affecting powder fluidization. *Powder Technol.* **58**:1–10 (1989).
29. D. L. Johnson, N. A. Esmen, K. D. Carlson, T. A. Pearce, and B. N. Thomas. Aerodynamic behavior of lipid microtubule aerosols. *J. Aerosol Sci.* **31**:181–188 (2000).
30. I. Balashazy, T. B. Martonen, and W. Hofmann. Fiber deposition in airway bifurcations. *J. Aerosol Med.* **3**:243–260 (1990).
31. P. E. Morrow. Factors determining hygroscopic aerosol deposition in airways. *Physiol. Rev.* **66**:330–376 (1986).
32. T. B. Martonen. Analytical model of hygroscopic particle behavior in human airways. *Bull. Math. Biol.* **44**:425–442 (1982).
33. A. J. Hickey and T. B. Martonen. Behavior of hygroscopic pharmaceutical aerosols and the influence of hydrophobic additives. *Pharm. Res.* **10**:1–7 (1993).
34. A. J. Hickey, I. Gonda, W. J. Irwin, and F. J. T. Fildes. The effect of hydrophobic coating upon the behavior of a hygroscopic aerosol powder in an environment of controlled temperature and relative humidity. *J. Pharm. Sci.* **79**:1009–1014 (1990).
35. S. P. Newman, A. Hollingworth, and A. R. Clark. Effect of Different Modes of Inhalation on Drug Delivery from a Dry Powder Inhaler. *Int. J. Pharm.* **102**:127–132 (1994).

36. H. Steckel and B. W. Müller. In Vitro Evaluation of Dry Powder Inhalers I: Drug Deposition of Commonly Used Devices. *Int. J. Pharm.* **154**:19–29 (1997).
37. A. H. de Boer, D. Gjaltema, and P. Hagedoorn. Inhalation Characteristics and their Effects on In Vitro Drug Delivery from Dry Powder Inhalers Part 2: Effect of peak flow rate (PFIR) and inspiration time on the in vitro release from three different types of commercial dry powder inhalers. *Int. J. Pharm.* **138**:45–56 (1996).
38. B. J. Meakin, J. M. Cainey, and P. M. Woodcock. Drug delivery characteristics of Bricanyl Turbohaler dry powder inhalers. *Int. J. Pharm.* **119**:91–102 (1995).
39. Y. Fukunaga, T. Nishibayashi, M. Odomi, and M. J. Shott. Evaluation of a novel β -2 agonist dry powder inhaler formulation using the Clickhaler: An initial feasibility study. *Respiratory Drug Delivery VII*. R. N. Dalby, P. R. Byron, S. J. Farr, J. Peart, Serentec Press, Inc., Raleigh, North Carolina 425-428 (2000)